

A METAMATERIAL ABSORBER FOR THE X-BAND REGIME - DESIGN, FABRICATION AND CHARACTERIZATION

*A Project Report
submitted by*

K DURAI SANKAR

*in partial fulfillment of the requirements
for the award of the degree of
MASTER OF TECHNOLOGY*



**DEPARTMENT OF ELECTRICAL ENGINEERING
INDIAN INSTITUTE OF TECHNOLOGY MADRAS**

MAY 2014

THESIS CERTIFICATE

This is to certify that the thesis titled **A Metamaterial absorber for the X-Band regime - Design, fabrication and characterization**, submitted by **K Durai Sankar**, to the Indian Institute of Technology, Madras, for the award of the degree of **Master of Technology**, is a bonafide record of the research work done by him under our supervision. The contents of this thesis, in full or in parts, have not been submitted to any other Institute or University for the award of any degree or diploma.

Dr. V Subramanian
Project Guide
Professor
Microwave Laboratory
Dept. of Physics
IIT-Madras - 600 036

Dr. Sarathi R
Project Co-Guide
Professor
High Voltage Laboratory
Department of Electrical Engineering
IIT-Madras - 600 036

Place : Chennai
Date : Jun 2014

ACKNOWLEDGEMENTS

I take this opportunity to express my deepest gratitude to my project guides Dr. V Subramanian and Dr. Sarathi R for their valuable guidance and motivation throughout the project. I am very grateful to them for providing their valuable time to guide me during the project.

I would like to thank my parents and wife for their love and support, without which it would have been impossible for me to carry my work at IIT Madras. I am grateful to Raj Kumar and Lincy Stephen, Microwave laboratory, Department of Physics for their guidance and assistance in this project.

It is a privilege to be a student in IIT Madras. I express special thanks to all my teachers for all the academic insight obtained from them. I also acknowledge the excellent facilities provided by the institute to the students. I would like to thank all my college friends who made this stay at IIT Madras a pleasant and memorable one. Lastly, nothing would have been possible without the blessings and kindness, guidance of God at every step.

ABSTRACT

The extensive development of Electronic systems and telecommunications had lead to major concerns regarding electromagnetic pollution. Motivated by environmental questions and by a wide variety of applications, the quest for materials with high efficiency to migrate electromagnetic interferences (EMI) pollution has become a mainstream field of research. In the past, many EMI shields have been proposed and implemented using conductive metal to reduce EMI by reflection and absorption. The shields implemented by using metals are relatively rigid, bulky and heavy. In this project an attempt has been made to design and implement metamaterial based electromagnetic shield which resolves the disadvantages of metals based EMI shield.

This paper presents a compact single band, polarisation insensitive, wide angle of incidence with comparatively large bandwidth metamaterials based electromagnetic interference (EMI) shield. It explores the configuration of EMI shield in which a dielectric substrate is sandwiched between two patterns of copper metal layers. The structure is simulated in CST microwave studio and displays an absorption peak of 95% at 9.54 GHz resonant frequency. The verified optimal design is also fabricated and the experiment was performed to confirm with the simulation results.

TABLE OF CONTENTS

Acknowledgements

Abstract

List of tables

List of figures

Abbreviations

Notation

1	Introduction	11
2	Electromagnetic Shielding	12
	2.1 Electro Magnetic Interference (EMI).....	12
	2.2 Electro Magnetic Compatibility (EMC)	14
	2.3 Electromagnetic Shielding.....	14
	2.4 Theory of EMI shielding.....	15
	2.5 Shielding Efficiency (SE).....	16
3	Meta Materials	19
	3.1 What are Metamaterials?	19
	3.2 Negative Refractive Index.....	20
	3.3 Absorption theory.....	22
	3.4 Why MM for absorber application?	23
4	Design and Simulation	25
	4.1 Design consideration	25
	4.2 Design.....	26
	4.3 Simulation of unit cell.....	28

4.4 EM Parameters	29
4.5 Simulation of stacked structure.....	30
5 Experimental results.....	34
5.1 Experimental setup.....	34
6 Conclusion.....	38
References.....	39

LIST OF TABLES

Table 4.1: Parameter of MM absorber	27
Table 4.2: Effective parameters at resonance	30
Table 4.3: Variation of separation between unit cells in stack	33

LIST OF FIGURES

Figure 2.1(a): Shielded enclosure to contain radiated emissions	14
Figure 2.1(b): Shielded enclosure to exclude radiated emissions	15
Figure 2.2: Components of EMI shielding	16
Figure 3.1: Material parameter space characterized by electric Permittivity (ϵ_r) and magnetic permeability (μ_r).....	19
Figure 3.2: Negative refractive index metamaterial for microwaves consisting of alternating layers of thin-wire media and circular split-ring resonators (SRR).....	21
Figure 4.1: Proposed MM absorber structure	26
Figure 4.2: Dimension of MM absorber	27
Figure 4.3: Unit cell with boundary condition perfect electric conducting (PEC) and perfect magnetic conducting (PMC) boundary conditions are applied in y and x-direction	28
Figure 4.4: Absorptivity as function of frequency	29
Figure 4.5: Shielding efficiency components as function of frequency	29
Figure 4.6: Electromagnetic parameters	30
Figure 4.7: Front (a) and rear (b) view of stacked structure	31
Figure 4.8: Stacked structure with boundary condition perfect electric conducting (PEC) and perfect magnetic conducting (PMC) boundary conditions are applied in y and x-direction	31
Figure 4.9: Absorptivity as function of frequency	32
Figure 4.10: Shielding efficiency components as function of frequency	32
Figure 5.1: Front and rear side of the fabricated metastructure	34
Figure 5.2: Block diagram of the experimental setup for SE measurement	35
Figure 5.3: Experimental setup for SE measurement	35

Figure 5.4: Measured SE for single MM layer	37
Figure 5.5: Measured SE for three layer stacked configuration	37

ABBREVIATIONS

A	Absorptivity
A_{eff}	Effective Absorptivity
BC	Boundary Condition
CST	Computer Simulation Technology
dB	Decibel
EM	Electromagnetic
EMC	Electromagnetic Compatibility
EMI	Electromagnetic Interference
GHz	Giga Hertz
MM / MTM	Meta Material
MMA	Meta Material Absorber
MWS	Microwave Studio
NRI	Negative Refractive Index
PEC	Perfect Electric Conductor
PMC	Perfect Magnetic Conductor
R	Reflectivity
SE	Shielding Efficiency
SE_A	Shielding Efficiency due to Absorption
SE_M	Shielding Efficiency due to Multiple reflection
SE_R	Shielding Efficiency due to Reflection
SE_{dB}	Shielding Efficiency in dB
T	Transmitivity
VNA	Vector Network Analyzer

NOTATION

E	Electric field
H	Magnetic field
η_s	Intrinsic impedance of medium
η_0	Intrinsic impedance of free space
E_I	Incident electric field
E_R	Reflected electric field
E_T	Transmitted electric field
H_I	Incident magnetic field
H_R	Reflected magnetic field
H_T	Transmitted magnetic field
p	Average size of unit cell
P_I	Incident power
P_T	Transmitted power
d	Thickness of dielectric
λ	Wavelength
ϵ	Electrical permittivity
μ	Magnetic permeability
Z	Impedance
n	Refractive index
ω	Angular frequency
k	Wave vector

CHAPTER 1

Introduction

The experimental growth of wireless communication, portable communication devices are common sights in our daily life. Also, with the heavy reliance on wireless communications, an increasing number of base stations are expected to ensure good wireless coverage. Such a trend has posed potential electromagnetic interference (EMI) risk or radiation hazards for some buildings. The effect of rapid growth of Electronic industries and widespread of electronic equipments in communication, computers, automotive, biomedical, space and other purpose has led to exponential increase in Electro Magnetic Interference (EMI).

Today's one of the most common application is the indoor wireless systems. With the increasingly popularity and deployment, the electromagnetic signals interfere between devices. Thus, there is strict demand for effective and practical shielding solutions. Unless the electronic equipments are properly shielded in the design phase, the threat from EMI is going to be very severe. Electromagnetic interference (EMI) shielding refers to the reflection and/or absorption of electromagnetic radiation by a material, which thereby acts as a shield against the penetration of the radiation through the shield.

This work designs a metamaterial based absorber which consists of a bilayer unit separated by a dielectric substrate structure for shielding based application. The design is verified using CST Microwave Studio and then the results are obtained post fabrication of the optimized design. The MM absorber has an absorption peak of 95% at 9.54 GHz. The absorber has a polarisation insensitive feature owing to its symmetric structure. These metamaterial based absorbers are promising candidates for thermally based imaging due to the relatively low volume, low density and narrow band response.

CHAPTER 2

Shielding basics

2. Electromagnetic Shielding

2.1 Electro Magnetic Interference (EMI)

When electromagnetic energy from sources external or internal to electrical or electronic equipment affects that equipment adversely by causing it to have undesirable responses, such as degraded performance or malfunctions, the electromagnetic energy is called electromagnetic interference (EMI) and the adversely affected equipment is said to be susceptible to EMI [1].

EMI is conducted via signal lines, antenna leads, power cables, and even ground connections, between EMI sources and EMI susceptible equipment.

EMI is coupled between components, circuits, or equipment having some mutual impedance through which currents or voltages in one circuit can cause currents or voltages in the other circuit. The mutual impedance may be conductive, capacitive, inductive, or any combination of these. Conductive coupling frequently manifests itself as common-mode interference through a ground return used in common by two circuits. Capacitive coupling may similarly cause common-mode interference between two circuits that are not nominally connected. Inductive coupling may exist between two circuits having self-inductive elements, if mutual inductance exists between them.

EMI is radiated through openings of any kind in equipment enclosures in the form of ventilation, access, cable or meter holes around the edges of doors, hatches, drawers, and panels and through imperfect joints in the enclosures. EMI may also be radiated from leads and cables leaving a source, or picked up by leads and cables entering a susceptible device. Any good radiator of electromagnetic energy is also a good absorber of electromagnetic energy and that an EMI source can also be susceptible to EMI from another source.

2.2 Electro Magnetic Compatibility (EMC)

EMC is defined as the capability of electronic equipment or systems to be operated in the intended electromagnetic environment at design levels of efficiency. A system is electromagnetically compatible with its environment if it satisfies three criteria:

- i. It does not cause interference with other systems.
- ii. It is not susceptible to emissions from other systems.
- iii. It does not cause interference with itself.

2.3 Electromagnetic Shielding

In this paper we will consider the radiation emission alone. Radiated emission can be controlled by containing the emission or by exclusion of radiated emission as shown in figure 2.1 (a) and (b) respectively. The most popular means to reduce the effect of EMI is by employing electromagnetic shield. An electromagnetic shield can be defined as housing, screen, or other object, usually conducting, that substantially reduces the effect of electric or magnetic fields between the source and the victim. The main purpose of the EMI shield is reduction of the electromagnetic field in a prescribed region of interest.

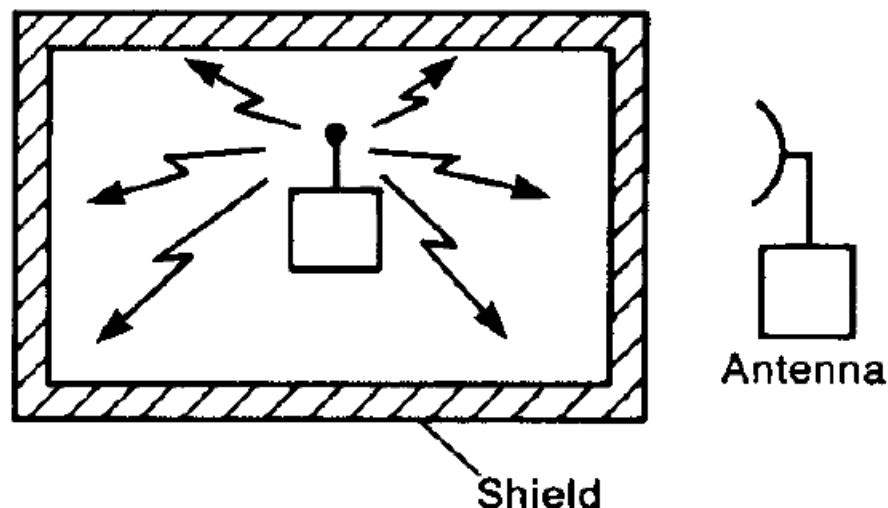


Figure 2.1(a): Shielded enclosure to contain radiated emissions

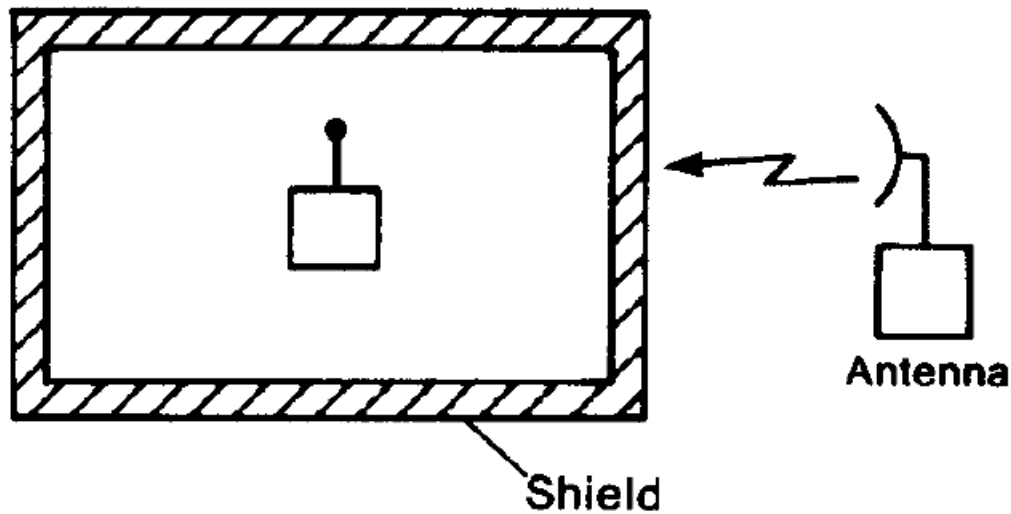


Figure 2.1(b): Shielded enclosure to exclude radiated emissions

2.4 Theory of EMI shielding

When an electromagnetic plane wave (E_i) is incident on a shielding material having different intrinsic impedance than the medium in which the EM plane wave was propagating, it undergoes reflection and transmission at the interface ($x=0$) thus creating a reflected wave (E_R) and a transmitted wave (E_{I-R}), at the external surface [2]. The amplitude of the E_R and E_{I-R} waves depend on the intrinsic impedance of the shielding material(η_s) and the EM incident wave propagating medium(η_0).

The transmitted wave (E_{I-R}) then travels into the internal shield, the amplitude of the wave decreases exponentially due to absorption. When the wave encounters the second interface at $x=d$, the part of wave incident will be transmitted out of the shield and a portion will be reflected in a shield. If the shield is thicker than the skin depth, the reflected wave from the internal surface will be absorbed by the conductive material, and thus multiple-reflection can be ignored. However, if the shield is thinner than the skin depth, the influence of multiple-reflection will be significant in decreasing overall EMI shielding.

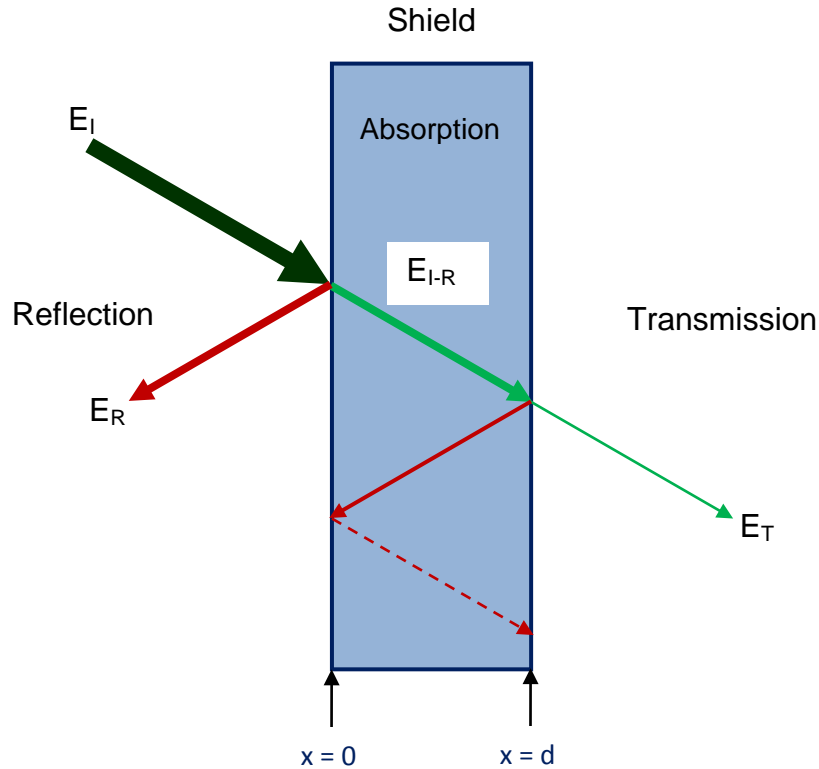


Figure 2.2: Components of EMI shielding

2.5 Shielding Efficiency (SE)

A shield is, conceptually, a barrier to the transmission of electromagnetic fields. We may view the effectiveness of a shield as being the ratio of the magnitude of the electric (magnetic) field that is incident on the barrier to the magnitude of the electric (magnetic) field that is transmitted through the barrier. Alternatively, we may view this as the ratio of the electric (magnetic) field incident on the product's electronics with the shield removed to that with the shield in place. Thus shield prevents coupling of undesired radiated electromagnetic energy into equipment otherwise susceptible to it.

$$\text{SE defined for electric field in dB} = 20 \log_{10} \left(\frac{E_I}{E_T} \right)$$

$$\text{SE defined for magnetic field in dB} = 20 \log_{10} \left(\frac{H_I}{H_T} \right)$$

Also, EMI SE (in terms of power) is the logarithm of ratio of the transmitted power when there is no shield (P_I) to the power when there is a shield (P_T).

$$SE = 10 \log_{10} \left(\frac{P_I}{P_T} \right)$$

For a single layer shield, the total SE has three components due to contributions from reflection (SE_R), absorption (SE_A) and multiple reflections (SE_M) [3]. The additional effects of multiple reflections inside shielding barrier need not be considered when $SE_A > 15\text{dB}$.

$$SE_{dB} = SE_R + SE_A + SE_M$$

$$\text{SE by reflection } SE_R = 20 \log_{10} \left(\frac{\eta_0}{4\eta_s} \right)$$

$$\text{SE by absorption } SE_A = 20 \log e^{d/\delta}$$

$$\text{SE by multiple reflection } SE_M = 20 \log \left| 1 - e^{-2d/\delta} \right|$$

The S_{11} and S_{12} are the scattering parameters (S-parameters) of the two-port vector network analyzer (VNA) system representing the reflection and transmission coefficients, respectively [4]. The transmittance (T), reflectance (R), and absorbance (A) through the shielding material are related to the S parameters as follows:

$$R = |S_{11}|^2$$

$$T = |S_{21}|^2$$

$$A = 1 - (R + T)$$

The SE_M is a correction term whose value may be positive, negative or zero. The effect of multiple reflections between both interfaces of the material is negligible when $SE_A \geq 10 \text{ dB}$. Therefore, the relative intensity of the effectively incident EM wave inside the materials after reflection is based on $(1 - R)$. Therefore, the effective absorbance (A_{eff}) can be described as $A_{eff} = \frac{1-(R+T)}{(1-R)}$ with respect to the power of the effectively incident EM wave inside the shielding material.

$$SE_R = 10 \log_{10}(1 - R) \text{ in } dB$$

$$SE_A = 10 \log_{10}(1 - A_{eff}) \text{ in } dB$$

$$= 10 \log_{10} \frac{T}{(1-R)}$$

CHAPTER 3

Basics of Meta Materials

3. Meta Materials

3.1 What are Metamaterials?

Before researching the technical aspects of metamaterials, we shall first define the meaning and scope of the word. The prefix “meta” comes from Greek and means “after” or “beyond”. In English it is used to either denote that something has occurred later, derived from a transformation, is a more highly organized or specialized form of, or transcends something else [5]. Thus with that in mind, a metamaterial is expected to display one or more properties rather qualitatively different - some investigators claim “extraordinary” than those of its “ordinary” constituents.

Metamaterials, artificial composite structures with exotic material properties, have emerged as a new frontier of science involving physics, material science, engineering and chemistry. In general, metamaterial is a metallic or semiconductor substance whose properties depend on its inter-atomic structure rather than on the composition of the atoms themselves. The property of a classical bulk material is essentially determined by the chemical elements and bonds in the material. Existing materials only exhibit a small subset of electromagnetic properties theoretically available but metamaterials can have their electromagnetic properties altered to something beyond what can be found in nature such as negative index of refraction, zero index of refraction, magnetism at optical frequencies etc.

Leading authors in the field of metamaterials have suggested adding another constraint in order to differentiate Electro Magnetic Metamaterials (EM-MTM) from other closely related optical devices such as photonic crystals [6]. The average size p of a unit cell also known as “meta-atom” in an EM-MTM should be much smaller than the driving wavelength of light ($p \ll \lambda$). Some authors go further as to propose a rule of thumb to clearly discriminate EM-MTM devices via an effective homogeneity condition ($p \leq \lambda$). The rationale behind that distinction is that EM-MTM is effectively homogeneous media for

incident radiation. While classical diffractive components like photonic crystals, whose cellular dimensions are typically integer multiples of a half-wavelength ($p \approx n \lambda/2$), cannot be considered as homogeneous. Hence cannot be characterized by a single value of the refractive index. In the case of photonic crystals, the waves scatter at each layers of the photonic crystal and interfere constructively in the Bragg regime [6]. At the early stage most research focused on metamaterials in the microwave region to implement artificial magnetism, artificial dielectrics, negative refractive index, and super lens [7]. Within past few years, metamaterials have rapidly advanced to terahertz and optical frequencies.

3.2 Negative Refractive Index

The refractive index n of an electromagnetically sensitive material depends on its constitutive parameters, the relative permittivity (ϵ_r) and the relative permeability (μ_r) through the relation $n = \pm \sqrt{\epsilon_r \mu_r}$. When a single constitutive parameter is negative, the refractive index is pure imaginary which results in lossy evanescent wave propagation in the medium as depicted in the areas 2 and 4 of Figure 3.1. When both constitutive components are either positive or negative, free wave propagation is enabled (areas 1 and 3). The doubly positive case (area 1) refers to the usual forward wave propagation in common dielectrics with positive refractive index. The doubly negative case (area 3) relates to the so called left-handed (LH) materials or negative refractive index (NRI) materials, characterized by a wave propagating with a phase velocity in the opposite direction of the energy flux (Poynting vector), hence labeled as “backward wave”. NRI materials and LH media were first theoretically predicted in 1968 by Victor Veselago [8]. In many published implementations of NRI materials, alternating MTM layers of negative ϵ_r (thin-wire media made of metallic nanorods) and layers of negative μ_r (Split Ring Resonators) are periodically stacked to create a globally NRI-MTM as shown in Figure 3.2.

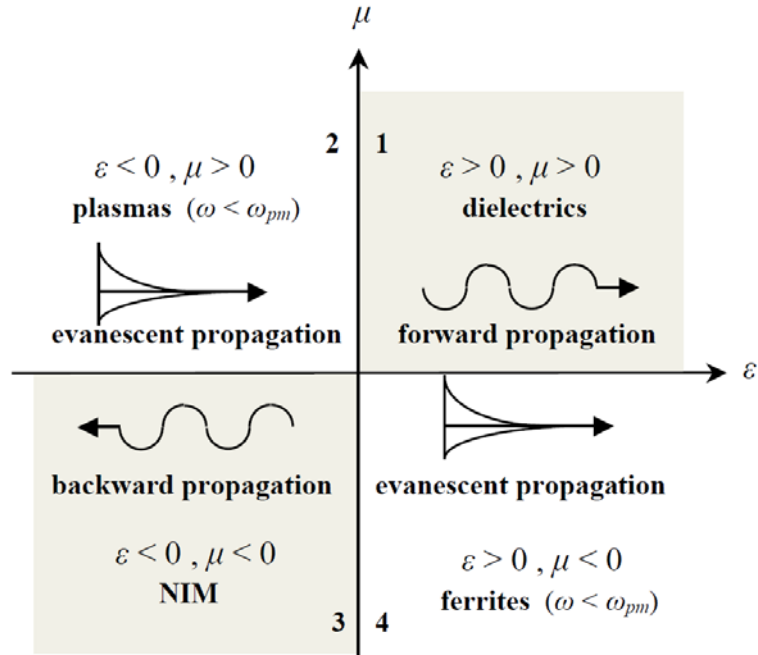


Figure 3.1: Material parameter space characterized by electric Permittivity (ϵ_r) and magnetic permeability (μ_r).



Figure 3.2: Negative refractive index metamaterial for microwaves consisting of alternating layers of thin-wire media and circular split-ring resonators (SRR).

3.3 Absorption theory

A near unity absorber is a device in which all incident radiation is absorbed at the operating center frequency [9]. The absorptivity $A(\omega)$ of the meta surface is expressed in terms of transmission $T(\omega)$ and reflectance $R(\omega)$ as $A(\omega) = 1 - T(\omega) - R(\omega)$. For unity absorption ($A(\omega) = 1$), the reflection (R) and transmission (T) should be ideally zero ($R=T=0$), thus the power of the impinging wave is mostly absorbed in the absorber materials. The transitivity and reflectivity are dependent on complex index of refraction $n(\omega) = n_1 + in_2$ and impedance $Z(\omega) = Z_1 + iZ_2$ for a slab length of d as

$$S_{21} = S_{12} = \frac{1}{\cos(nkd) - \frac{i}{2}\left(Z_r + \frac{1}{Z_r}\right)\sin(nkd)}$$

$$S_{11} = S_{22} = \frac{i}{2}\left(\frac{1}{Z_r} - Z_r\right)\sin(nkd)$$

Where:

$$Z_r = \sqrt{\frac{(1+S_{11})^2 - S_{21}^2}{(1-S_{11})^2 - S_{21}^2}}$$

$$R = |S_{11}|^2, T = |S_{21}|^2$$

Thus the condition for unity absorption is

$$Z_r \rightarrow 1 \Rightarrow Z = Z_0; \Rightarrow R \rightarrow 0 \text{ and } T \rightarrow 0$$

$$i.e. T = e^{-2n_2kd}; \quad \lim_{n_2 \rightarrow \infty}(T) = 0$$

The combined dielectric ($\epsilon_r = \epsilon_{real} + \epsilon_{imaginary}$) and magnetic losses in the system $\mu_r = \mu_{real} + \mu_{imaginary}$ are characterized by imaginary part of n . Therefore the physical interpretation of the above derivation is that (in the absence of reflections) the transmission of an electromagnetic wave with a wave vector k through a slab of thickness d is determined entirely by losses in the slab. To create a very high absorber it is then necessary for $Z=1$ at a point where n_2 is large. The higher the value of n_2 that can be obtained, the thinner the slab can be in the propagation direction. In this manner, one can overcome the quarter-wavelength thickness requirement of traditional Salisbury screens and Jaumann absorbers. Thus precise control of n and Z is necessary to realize

a high absorber. The permeability and permittivity are characterized by a real part (which describes propagation in a medium) and an imaginary part (which describes absorption and loss in a medium), perhaps manipulating the imaginary component of ϵ and μ to be simultaneously large over a given frequency range and thus absorb both the incident electric and magnetic fields well.

3.4 Why MM for absorber application?

- i. Since the mechanism of absorption can be achieved through impedance matching and the loss. Metamaterials based absorbers permit construction of complex materials by tailoring the electromagnetic parameters like electric permittivity(ϵ) and magnetic permeability(μ). The electromagnetic properties can be engineered by variation in the metamaterial geometry [7].
- ii. Design demonstrated in a particular band of Electro Magnetic spectrum can be made to operate in some other band by optimizing the geometry of the metamaterial structure.
- iii. In contrast to conventional absorbers which are limited to microwave and lower frequencies, the metamaterial based absorbers can be used at Near IR and optical wavelengths.
- iv. Unlike Frequency Selective Surfaces (FSS) which offers tuning of single impedance (Z) parameter, metamaterial absorber permits tuning of electric permittivity(ϵ) and magnetic permeability(μ). Control over the complex Electromagnetic parameters permits adjustment in quality factor, modifies losses of the constituent materials.
- v. Polarisation independence can be achieved by utilizing structures with four fold rotational symmetry or employing equal combination of polarisation dependent unit cells rotated by 90 degrees with respect to each other or by using chiral version of metamaterial. Metamaterial based absorbers can achieve high absorptivity at broad angle of incidence for both TM and TE incidence of EM Wave in addition to polarisation property of metamaterial.

- vi. Comparatively broad Bandwidth (BW) can be realized by creating unit cells with matched impedance at multiple frequencies that are close enough to create a broadband single peak or by introducing lumped elements such as resistances and capacitances in the MM structures. Dynamic/Tunable absorbance can be achieved by integrating microwave diodes into the metamaterial array and biasing the Varactor Diodes at different levels.
- vii. Spatial dependence can be accomplished by arranging unit cells such that at predetermined area, exhibit near unity absorbance while those in other areas with unit cells that exhibit near zero absorbance.
- viii. In contrast to conventional absorbers that require a thickness of at least $\lambda_0/4$, metamaterial absorbers can be relatively very thin even up to the order of $\lambda_0/75$. In certain applications it provides the ability of the metamaterial absorber to be highly flexible.
- ix. Availability of many commercial simulation programs like CST Microwave Studio, HFSS and Comsol which yield good match between simulated and experimental results. Above all, the metamaterial offers low volume, low density, low weight and low cost.

CHAPTER 4

Design and Simulation

4. Design

4.1 Design consideration

Various configurations have been proposed for metamaterial based configuration of the metal and the dielectric layers are employed. A configuration with two copper layers separated by a dielectric substrate is the most popular of the available design. In many cases the bottom layer is completely copper laminated called ground plane while the top layer has periodic arrangement of patterns [10]. Many patterns like cross, split wire, Jerusalem cross, square patch, circular or square rings, hexagonal have been reported [11]. Few cases of the MM based absorbers have reported periodic pattern of copper patterns on both top and bottom layers [12, 13].

The wave vector is perpendicular to the top and bottom plane containing the metal pattern in the Z direction. The electric component of EM wave is parallel with the X-axis and the magnetic component is parallel with the Y-axis. In either of the MM absorber configurations, when EM wave is incident on the structure, the electric field is coupled with the top periodic resonator structure which controls the value of electrical permittivity (ϵ) and the anti parallel current between the top and bottom layer can be coupled with the magnetic field which controls the magnetic permeability (μ). The electric and the magnetic fields can be highly coupled by optimally adjusting the physical parameters of the top and bottom layer along with fine tuning of the dielectric substrate thickness. The above tuning can be achieved in a particular frequency range where the surface impedance (η_s) can be matched with free space impedance (η_0). The absorption can be maximized by minimizing both reflected power and transmitted power. For materials with complex permittivity (ϵ) and magnetic permeability (μ), the total loss depends on the imaginary part of both refractive index and surface impedance.

$$Z(\omega) = \sqrt{\frac{\mu_r \mu_0}{\epsilon_r \epsilon_0}} = \eta_0 \sqrt{\frac{(1 + S_{11})^2 - S_{21}^2}{(1 - S_{11})^2 - S_{21}^2}}$$

$$n(\omega) = \frac{1}{kt} \cos^{-1} \left[\frac{1}{2S_{21}} (1 - S_{11}^2 + S_{21}^2) \right]$$

4.2 Design

In this paper the MM based absorber structure consists of a metal-dielectric-metal configuration. The top and bottom plate design consists of copper metal based periodic structures. The dielectric (FR4 lossy substrate) is sandwiched between the top and bottom metallic surface (Perfect Electric Conductor). The rear structure as shown in figure 4.1 has four fold rotational symmetry about the propagation axis and hence polarisation insensitive while the front structure is a closed square loop. This design also permits a wide angle on incidence of the incident EM wave without much degradation in the absorber performance. The thickness of copper metal layers and FR4 dielectric is $35 \mu m$ and $0.8 mm$ respectively. The specification and the dimensions (top (4.2a), bottom (4.2b) and side (4.2c) views) of the MM absorber is listed in table 4.1 and figure 4.2.

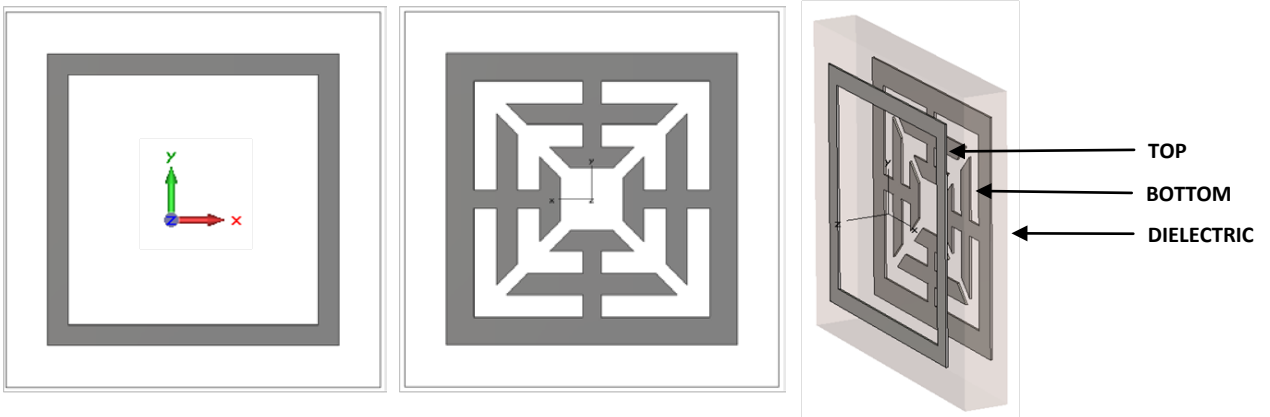


Figure 4.1: Proposed MM absorber structure

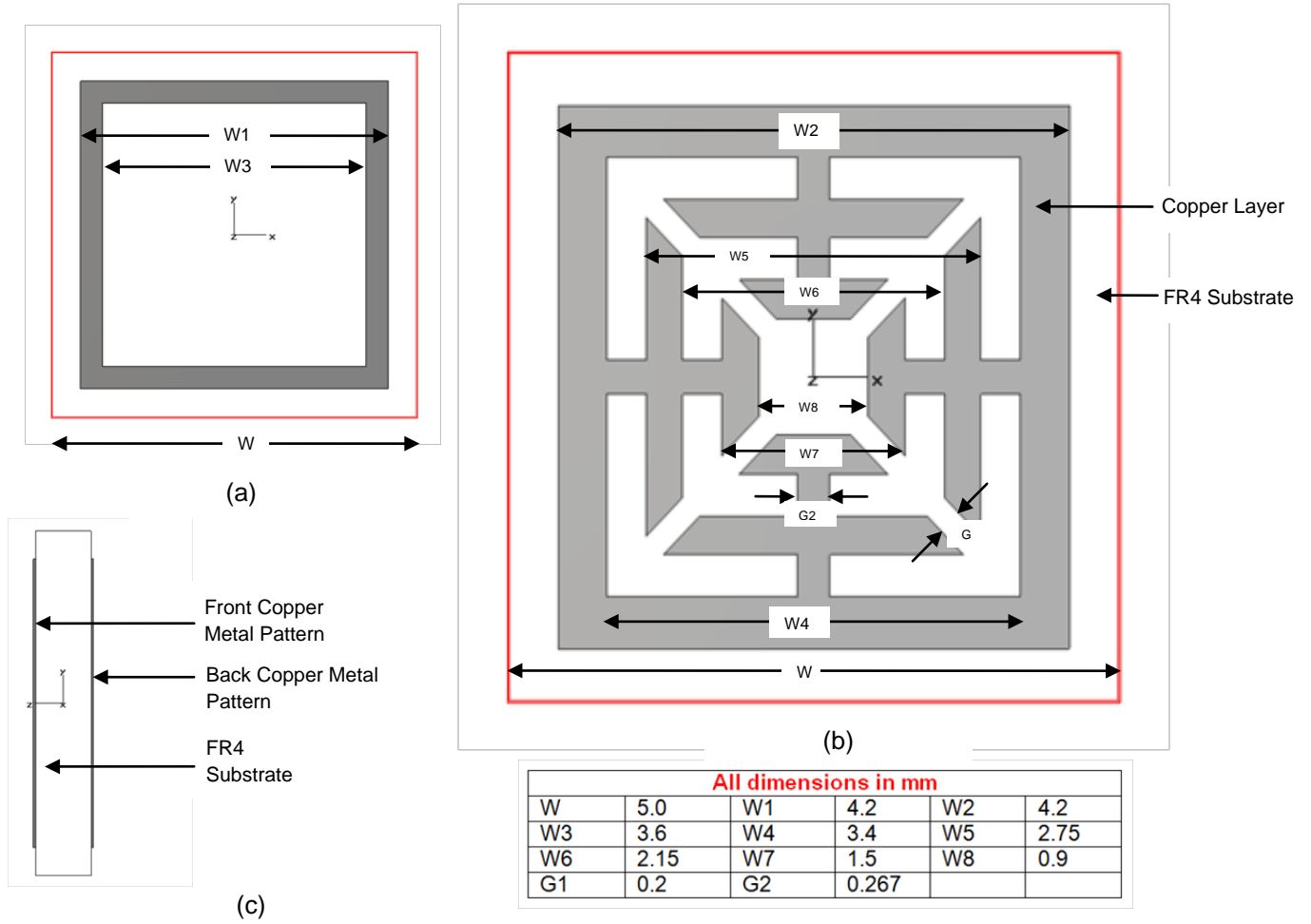


Figure 4.2: Dimension of MM absorber

PARAMETER	VALUES
Copper Metal Thickness	0.035 mm
FR4 Substrate thickness	0.8 mm
FR4 SPECIFICATION	
Material	Lossy
Type	Normal
Relative permittivity	0.43
Relative permeability	1
Tan delta	0.025

Table 4.1: Parameter of MM absorber

4.3 Simulation of unit cell

The simulation is done on metamaterial unit cell using CST Microwave Studio by setting up appropriate boundary conditions and port excitations. Perfect Electric and Perfect magnetic boundary conditions with waveguide ports on either sides of the structure were used in the simulation to compute the scattering parameters S_{11} and S_{21} as shown in figure 4.3.

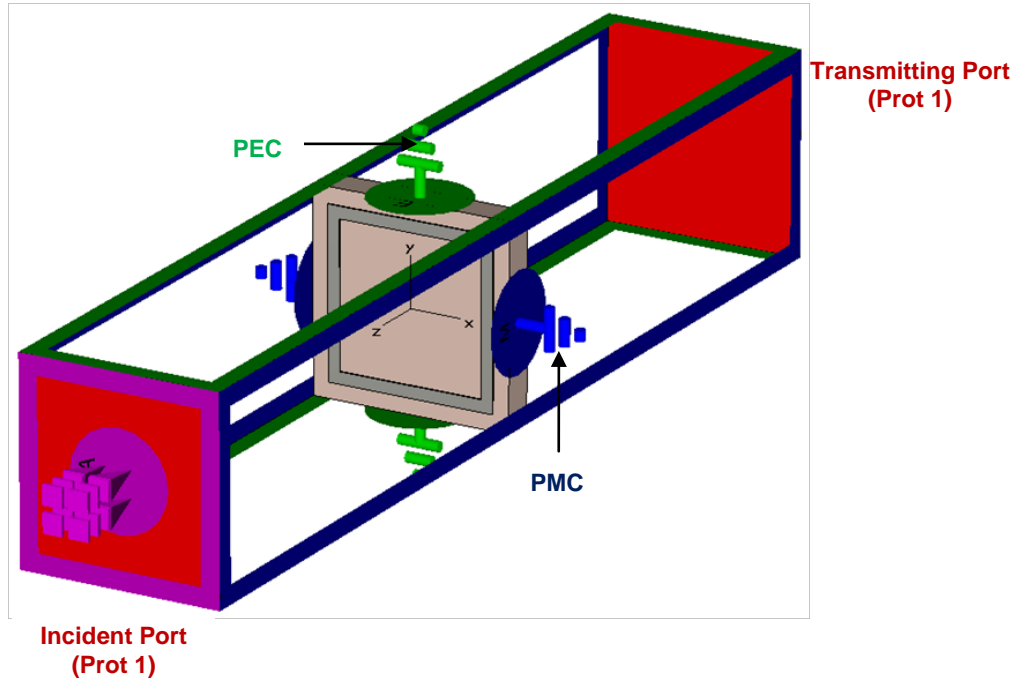


Figure 4.3: Unit cell with boundary condition perfect electric conducting (PEC) and perfect magnetic conducting (PMC) boundary conditions are applied in y and x-direction respectively

The maximum absorptivity of 94.75% is observed at 9.54 GHz. The absorptivity and components of shielding efficiency of the designed metamaterial unit cell at normal incidence as a function of frequency obtained in the simulation is presented in figure 4.4 and figure 4.5 respectively. The optimized parameters are those which are yielded at the lowest reflectivity at the design frequency of 9.5 GHz.

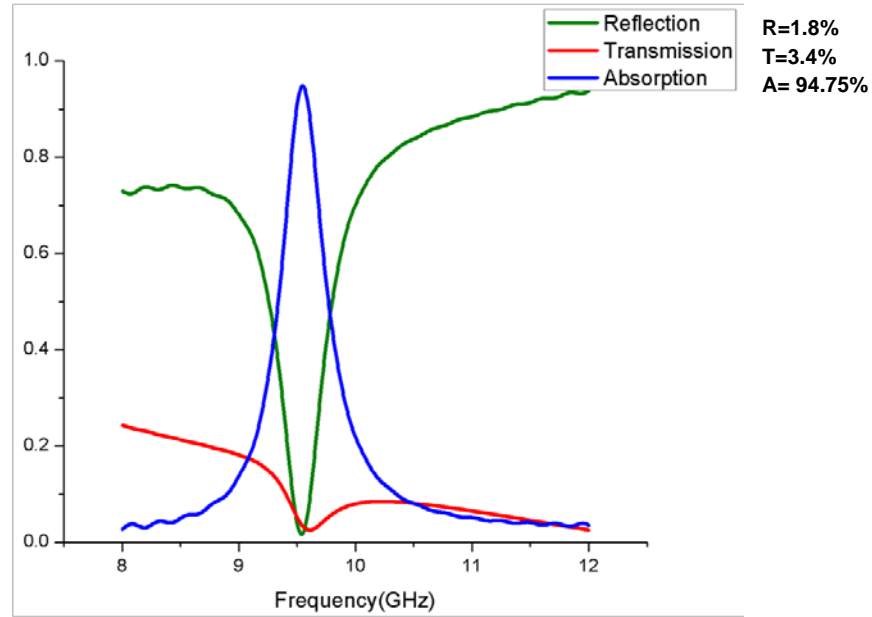


Figure 4.4: Absorptivity as function of frequency

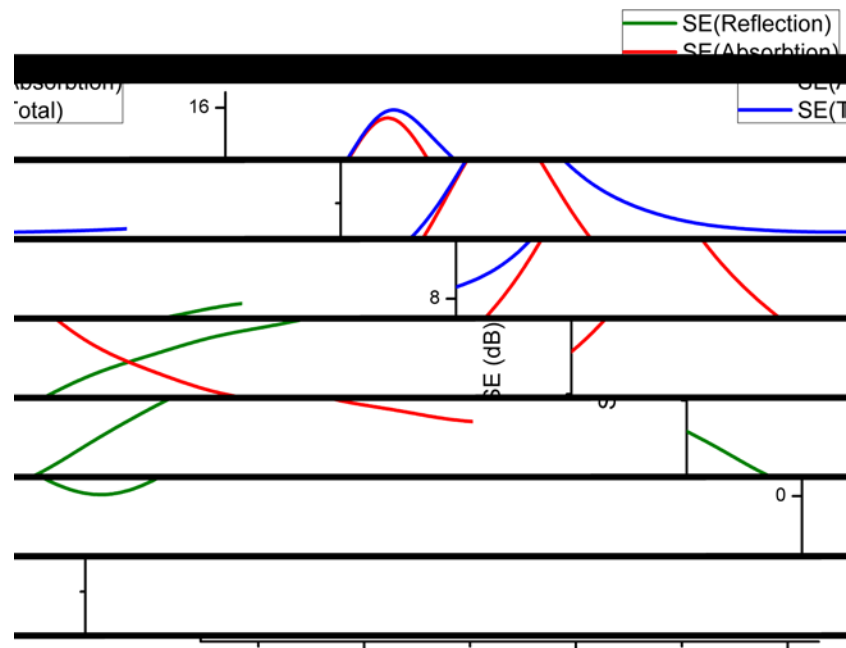


Figure 4.5: Shielding efficiency components as function of frequency

4.4 EM Parameters

The electrical permittivity ($\epsilon = \epsilon_1 + i\epsilon_2$), the magnetic permeability ($\mu = \mu_1 + i\mu_2$), refractive index ($n = n_1 + in_2$) and impedance ($Z = Z_1 + iZ_2$) parameters were retrieved

at the electrical and magnetic resonance is displayed in figure 4.6. The real part of (ϵ) and (μ) contributes towards the propagation of the EM wave while the imaginary part of (ϵ) and (μ) describe the loss. The values of impedance Z , (ϵ) and (μ) at resonance is shown in table 4.2. The large values of the imaginary part of (ϵ) and (μ) show that the losses are increased thereby maximizing the absorptivity. Also, the value of surface impedance is matched to the free space impedance of $Z_{10} = 377 \text{ Ohm}$.

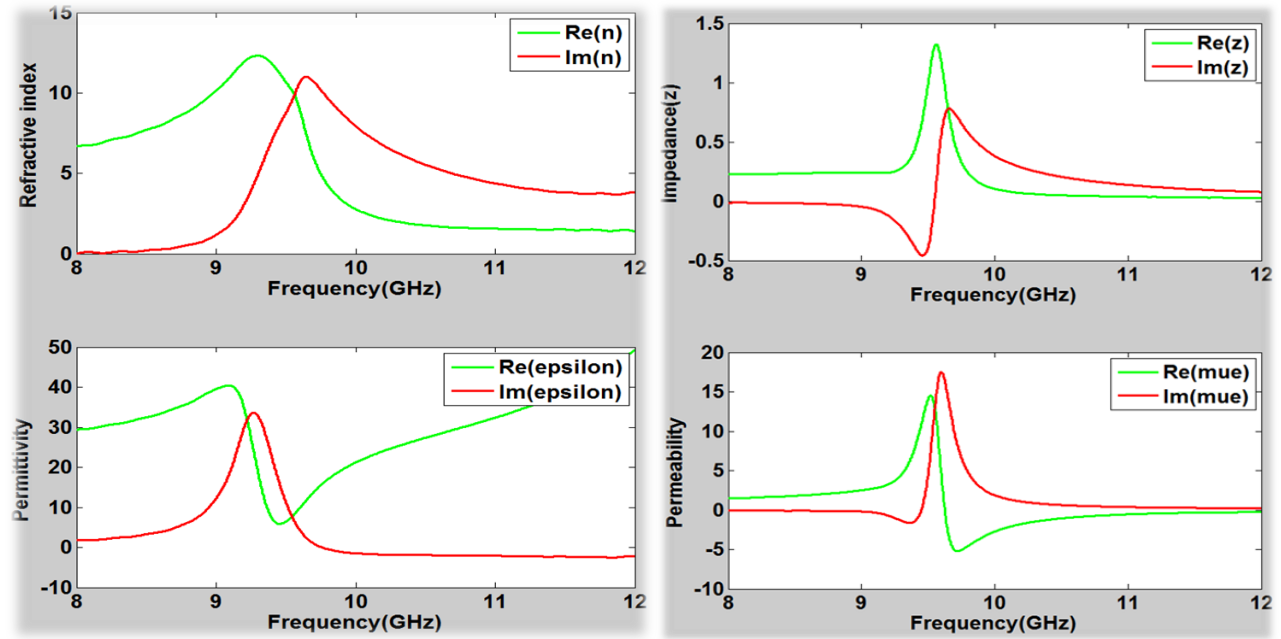


Figure 4.6: Electromagnetic parameters

Effective Parameters	Real	Imaginary
Permittivity ($\epsilon = \epsilon_1 + i\epsilon_2$)		
Permeability ($\mu = \mu_1 + i\mu_2$)		
Impedance ($Z = Z_1 + iZ_2$)		
Surface impedance (Z)		

Table 4.2: Effective parameters at resonance

4.5 Simulation of stacked structure

The simulation is done on metamaterial stacked structure with a distance (D) and air medium as the medium between individual unit cell with shown in figure 4.7 using CST Microwave Studio by setting up appropriate boundary conditions and port excitations. Perfect Electric and Perfect magnetic boundary conditions with waveguide

ports on either sides of the structure were used in the simulation to compute the scattering parameters S_{11} and S_{21} as shown in figure 4.8.

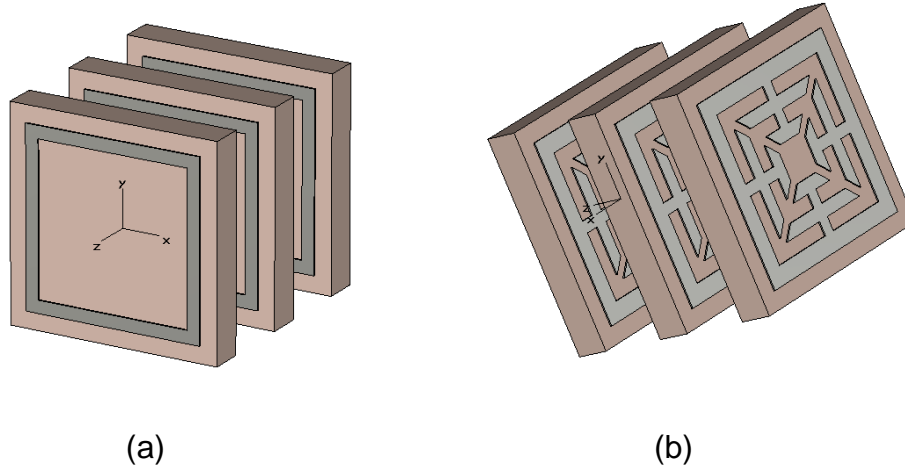


Figure 4.7: Front (a) and rear (b) view of stacked structure

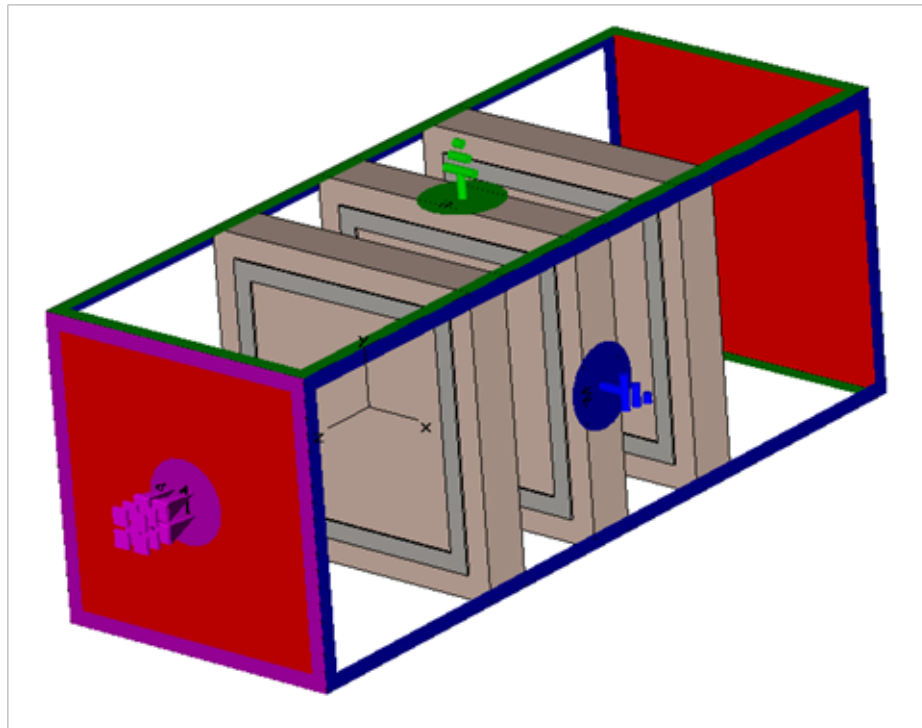


Figure 4.8: Stacked structure with boundary condition perfect electric conducting (PEC) and perfect magnetic conducting (PMC) boundary conditions are applied in y and x-direction respectively

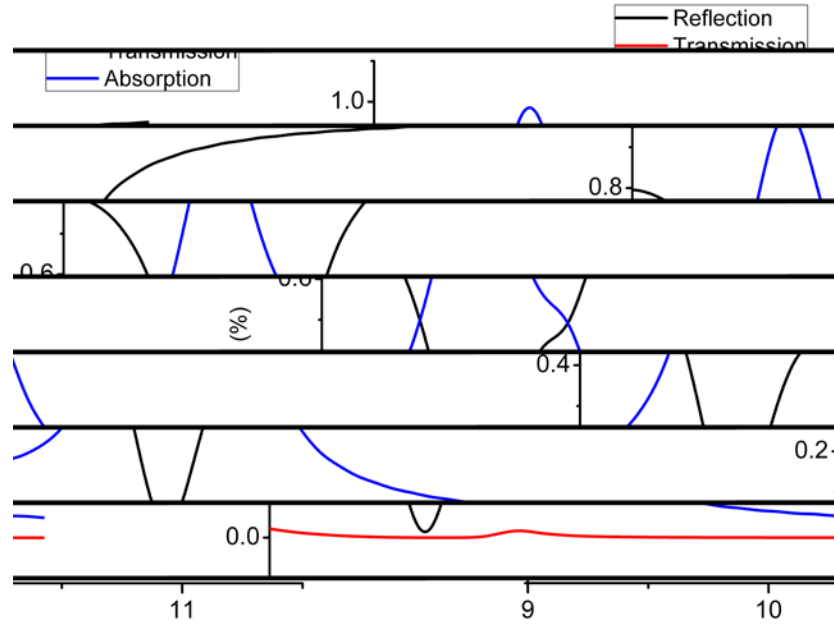


Figure 4.9: Absorptivity as function of frequency

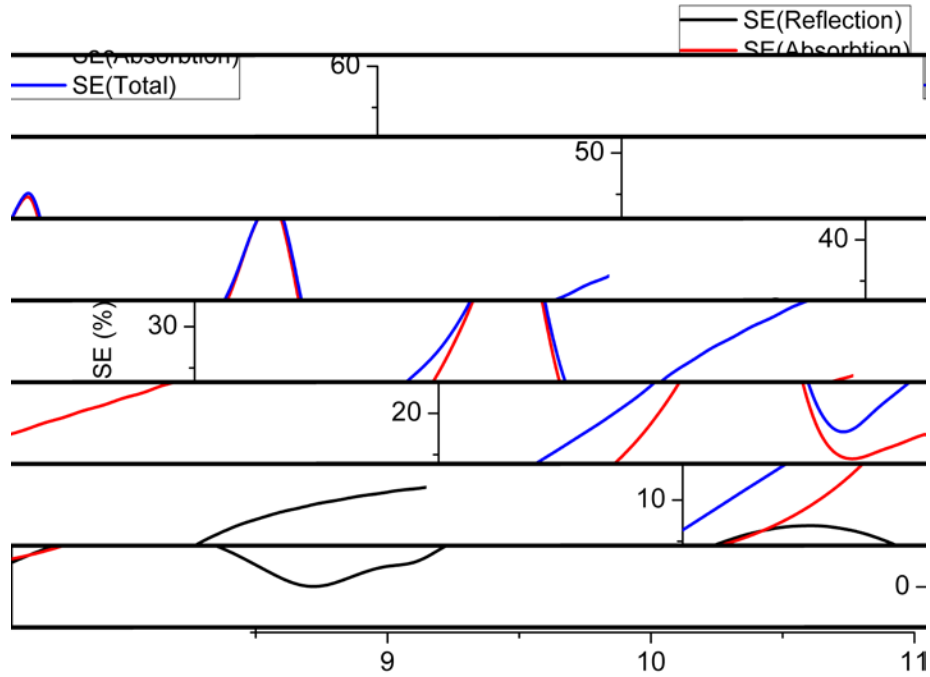


Figure 4.10: Shielding efficiency components as function of frequency

The maximum absorptivity of 98.6% is observed at 9.64 GHz compared to absorption of 94.5% in case of unit cell. The absorptivity and components of shielding

efficiency of the designed metamaterial stacked structure at normal incidence as a function of frequency obtained in the simulation is presented in figure 4.9 and figure 4.10 respectively. The shielding efficiency (SE) increased from 16 dB to 45 dB when the unit cell was stacked in the above configuration. The separation between the unit cells was varied and the parameters measured are shown in table 4.3. It is found that the absorption is maximum at a separation of 3.6 mm between the unit cells.

Gap (D)	R	T	A (%)
0.8	0.135498	0.000576	86.39
1.6	0.035231	0.000166	96.46
2.0	0.023901	0.000090	97.60
3.0	0.015901	0.000074	98.40
3.6	0.014376	0.000077	98.55
3.8	0.014957	0.000094	98.49

Table 4.3: Variation of separation between unit cells in stack

CHAPTER 5

Experimental results

5. Experiment

5.1 Experimental setup

After simulating the unit cell designed with optimized parameters, an array of 21 x 21 cells was fabricated using a surface micro machining process on FR4 substrate with a machining tolerance of 0.2mm. The enlarged view of the fabricated EMI shield (front and rear side) is shown in figure 5.1(a) and (b) respectively. The block diagram representation of the proposed experimental setup is displayed in figure 5.2.

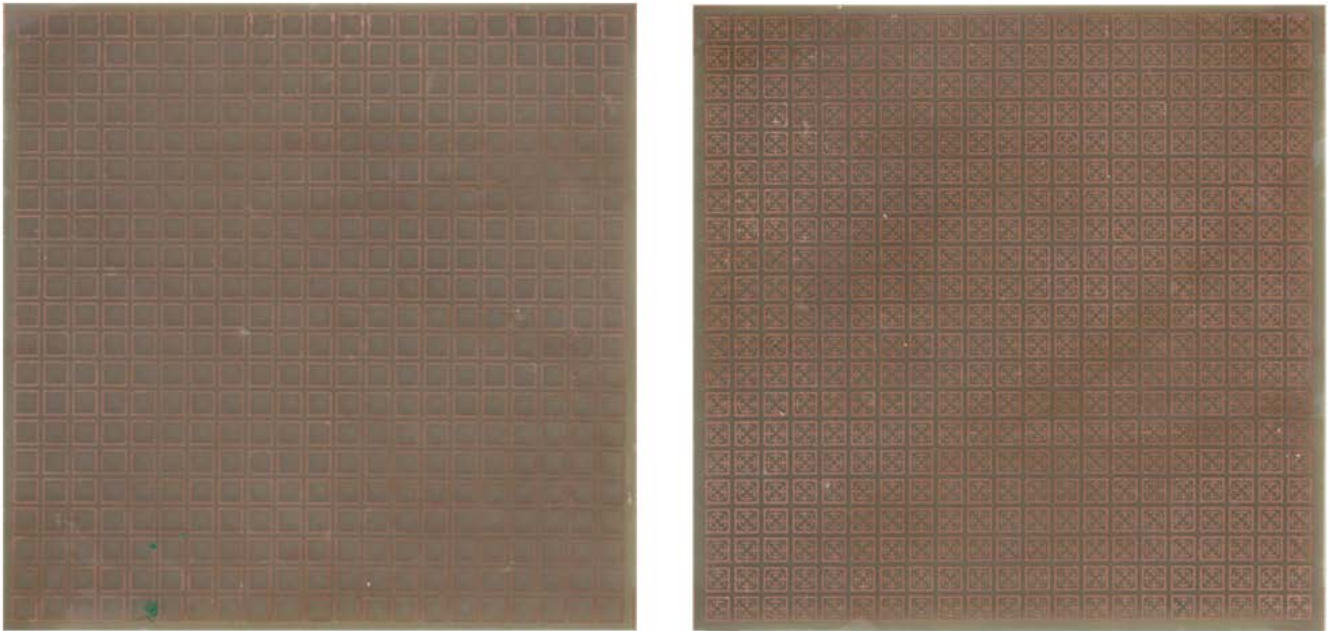


Figure 5.1: Front and rear side of the fabricated metastructure

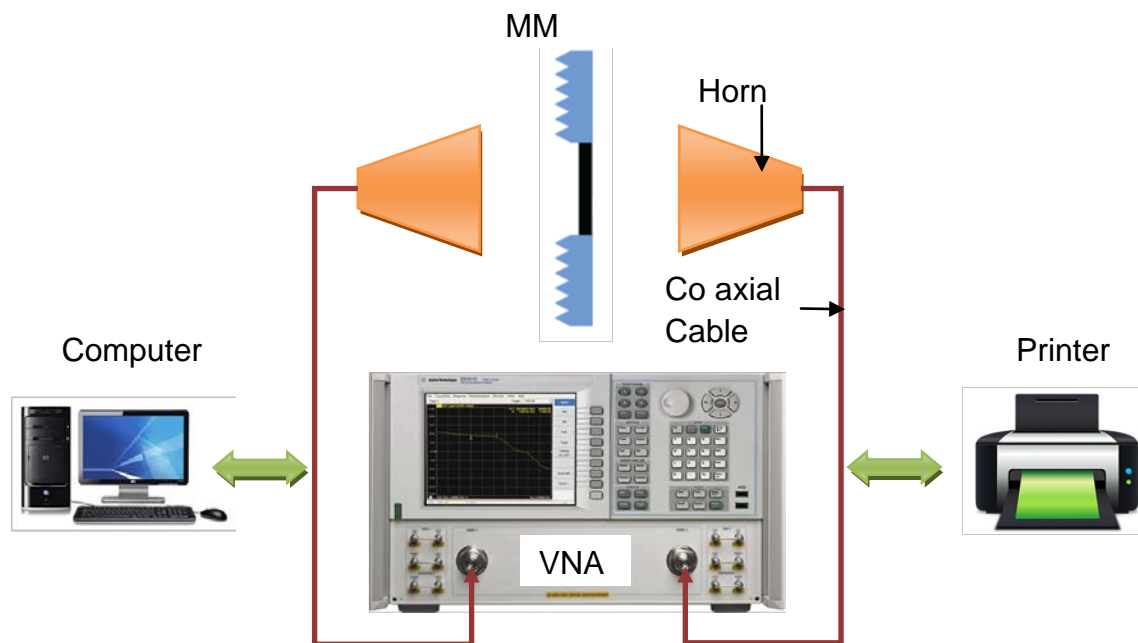
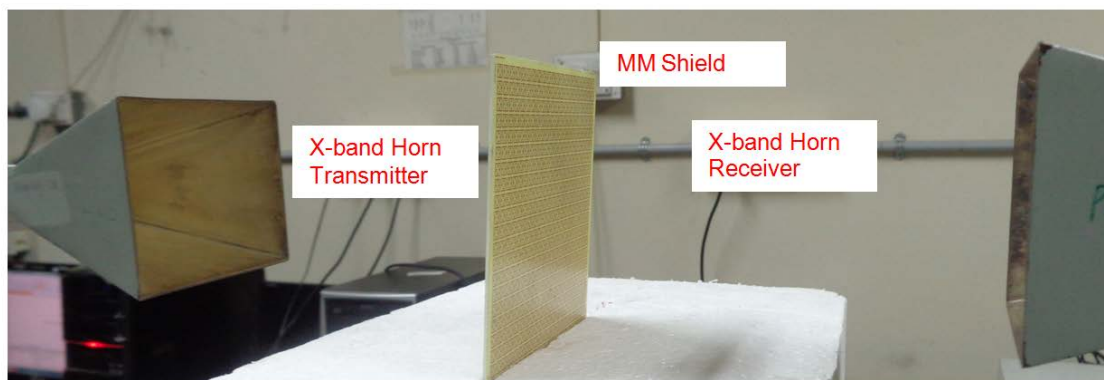


Figure 5.2: Block diagram of the experimental setup for SE measurement

The proposed experimental setup consists of a pair of X-band horn antenna (Make: Vidyut Yantra Udyog, Model: X5041) chosen to transmit and receive the EM wave propagating across the stop band shield for its directivity and antenna gain. The entire experiment is setup in the anechoic chamber designed for X-band applications. The distance between each antenna and the EMI shield is optimized for improving the S parameter measurement. The S parameters were not measured as the Agilent Vector Network Analyzer (VNA) available in the institute is unserviceable.

Alternately, the experiment to measure shielding efficiency was carried out utilizing a signal generator (Make: Agilent, Model: E8257D), power meter (Model: E4416A EMP-P series) and power sensor (Model: 8481D) along with the transmitter receiver horn antenna pair. The experimental setup is used for measurement of SE at normal incidence. The experiment was performed with the fabricated sample placed between the two X-band horn antennas (at the midpoint) separated at a distance of 50cm. The sample was held at a normal angle of incidence with the help of a clamp arrangement as shown in figure 5.3 and the measured results is shown in figure 5.4. A maximum of 27.5 dB of shielding was achieved at 10.05 GHz. The results for the three layer stacked configuration is shown in figure 5.5. It can be observed that immense increase in SE (48.3 dB at 10.5 GHz) is observed in the stacked configuration compared to that of single layer. The frequency shift in peak of measured SE in the single layer and three layer stacked configuration may be because of the additional reactance that arises due to arraying of unit cells and reactance between each layer of MM shield.



(a) Antenna arrangement



(b) Signal generator and power meter

Figure 5.3: Experimental setup for SE measurement

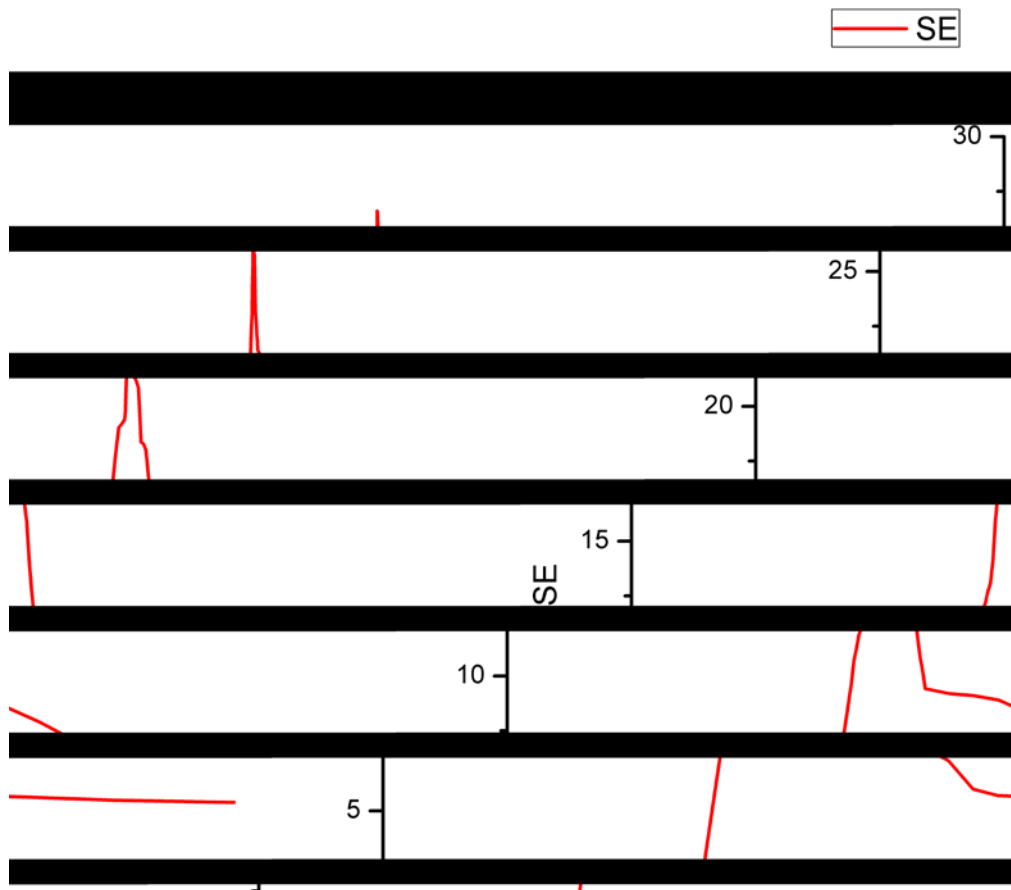


Figure 5.4: Measured SE for single MM layer

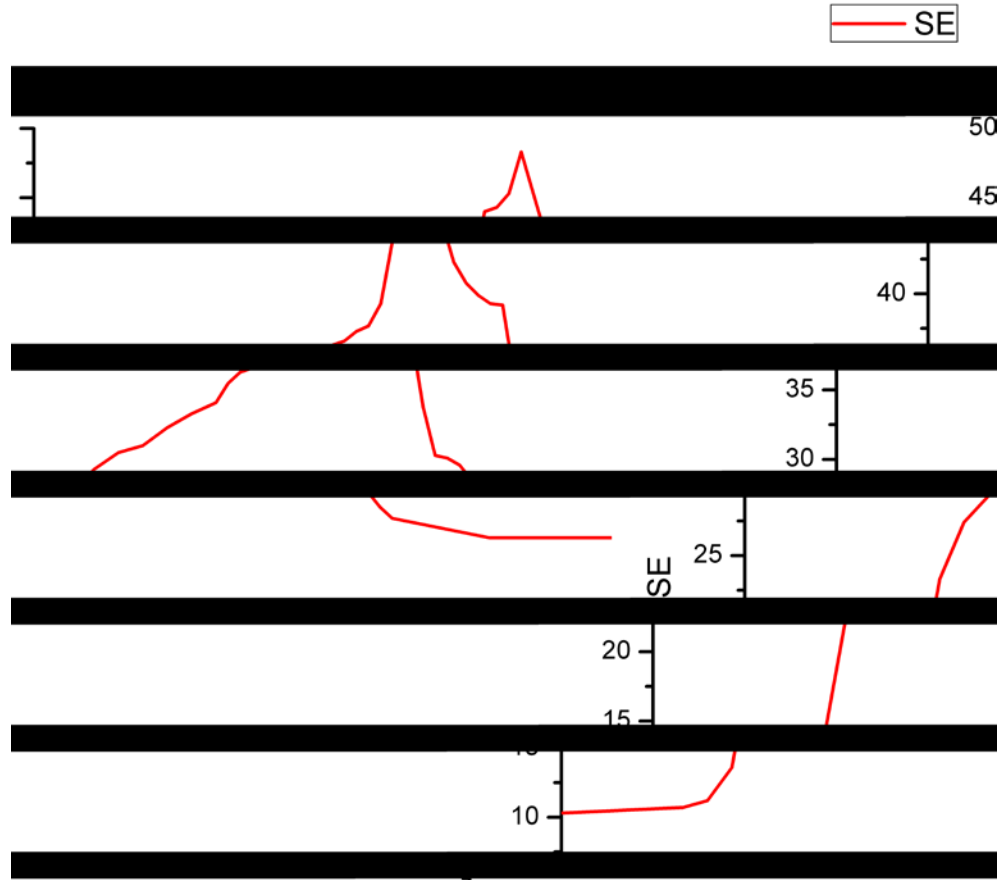


Figure 5.5: Measured SE for three layer stacked configuration

The deviation of experimental results from the simulated resonance absorption will not match. This may be because of scattering of radiation from imperfect edges arising from fabrication, fabrication tolerance of the micromachining setup and imperfection in measurement. Also, the imaginary part of electric permittivity $Im(\epsilon_r)$ is an uncertain parameter. So, the abnormal variation in $Im(\epsilon_r)$ might be another reason for error between the measured and simulated results. The response of the absorber could be further improved through refinement and optimization of the fabrication process.

CHAPTER 6

Conclusion

In this paper we have realized a metamaterial based absorber for the purpose of EMI shielding. The band stop resonant frequency is independent of polarisation and angle of incidence making it very suitable for practical EMI shielding applications. The proposed MM absorber consists of a FR4 dielectric substrate sandwiched between a square loop structure on the top and a patterned ground plane or resonator structure on the bottom. The simulation results show an absorption peak of 95% at 9.54 GHz resonant frequency. Good shielding efficiency is demonstrated through both simulation and measurement. The absorptivity can be improved by optimizing the fabrication process. This can be used in many applications like selective thermal emitters, detection and sensing, imaging, spectroscopy, integrated photonic circuits, solar cell etc.

REFERENCES

- [1]. **Clayton R Paul** - Introduction to EMC, A JOHN WILEY & SONS, INC. PUBLICATION
- [2]. **Mohammed H. Al-Saleh, Uttandaraman Sundararaj**, "Electromagnetic interference shielding mechanisms of CNT/polymer composites"
- [3]. **Parveen Sainia, Veena Choudharyb, B.P. Singhc, R.B. Mathurc, S.K. Dhawana**, "Polyaniline-MWCNT nanocomposites for microwave absorption and EMI shielding.
- [4]. **Jean-Michel Thomassin, Christine, Thomas Pardoen, Christian Bailly, Isabelle Huynen, Christophe Detrembleur**, "Polymer/carbon based composites as electromagnetic interference (EMI) shielding materials".
- [5]. Merriam-Webster Collegiate Dictionary 10th Edition.
- [6]. **Yongmin Liu and Xiang Zhang**, "Metamaterial: A new frontier of science and technology".
- [7]. **Bora Ung**, "Metamaterials: A metareview".
- [8]. **V.G. Vaselago**, "Electrodynamics of substances with simultaneous negative Electrical and Magnetic permeabilities".
- [9]. **Claire M. Watts, Xianliang Liu, Willie J. Padilla**, "Metamaterial electromagnetic wave absorber".
- [10]. **Saptarishi Ghosh, Debdeep Sarkar, Somak Bhattacharyya, Kumar Vaibhav Sriavstava**, "Design of ultra thin dual band microwave metamaterial absorber".
- [11]. **Christopher M. Bingham, Hu Tao, Xianliang Liu, Richard D. Averitt, Xin Zhang, Willie J. Padilla**, "Planar wallpaper group metamaterial for novel terahertz application".
- [12]. **Hu Tao, Nathan I. Landy, Christopher M. Bingham, Xin Zhang, Richard D. Averitt, Willie Padilla**, "Metamaterial for terahertz regime: Design, fabrication and characterization".
- [13]. **Nathan I. Landy, S. Sajuyigbe, D.R. Smith, W.J. Padilla**, "Perfect metamaterial absorber".

